

# COMPUTER SIMULATION FOR FINDING NONCLASSICAL PROPERTIES IN KERR NONLINEAR COUPLER WITH NONLINEAR EXCHANGE

Nguyen Thi Dung

Received: Received: 15 March 2017 / Accepted: 7 June 2017 / Published: July 2017

©Hong Duc University (HDU) and Hong Duc University Journal of Science

**Abstract:** *In this paper, we present the techniques of simulation modelling for quantum dynamics of Kerr nonlinear coupler system which consists of two nonlinear quantum oscillators mutually coupled by continuous nonlinear interaction. We show that by using evolution operator formalism we can model the quantum system and derive the “exact” solution for finding the existence of nonclassical properties in terms of squeezing, antibunching, intermodal entanglement and their higher order counterparts under the effect of dissipation process.*

**Keywords:** *Squeezing, antibunching, intermodal entanglement, nonclassicality.*

## 1. Introduction

Over last decades, there exists a rapid development of a particular interest in research of quantum correlations in multi-parties systems consisting of two or more subsystems. Such correlations are the significant problem from both the physical viewpoints and applications in quantum information theory [2,3,6,23]. These signature of nonclassicalities are related to different quantum features as squeezing, higher order squeezing, antibunching, higher order antibunching, intermodal entanglement, and higher-order entanglement. Squeezing can be defined in terms of the quadrature variance of a component, and used for the performance of continuous variable quantum information processing [6]. Antibunching can be defined by correlation function at zero delay. This phenomenon is used to build a high-quality single photon sources [23] and applied to perform quantum communication and quantum computation [6]. Entanglement plays an important role in implementation quantum cryptography, quantum teleportation, quantum key distribution [1,6,23]. Generation of those correlations in physical systems becomes one of the most important points. Therefore, finding physical models allowing for generating such states seems to be especially substantial. This paper aims to show how it is possible to

---

Nguyen Thi Dung  
Faculty of Natural Sciences, Hong Duc University  
Email: Nguyenthidung@hdu.edu.vn (✉)

generate non-classicalities by using techniques of simulation modeling for quantum dynamics of Kerr-like nonlinear coupler system under effect of damping process. Quantum Kerr-like nonlinearity models are widely discussed in numerous applications. For instance, they are considered as a source of non-Gaussian motional states of trapped ions [21], and are discussed in a context of the Bell's inequality violations [19]. Such models can also be applied in description of nanomechanical resonators and various optomechanical systems [20], Bose-Einstein condensates [18]. Thus, the modes of nonlinear directional coupler proved to be a promising device, easy treatment for finding numerical solutions and generating nonclassical effects and hence its quantumness.

## 2. The model description and simulation method

The considered system consists of two nonlinear Kerr-like oscillators mutually coupled by nonlinear interaction, where each oscillator corresponds to a single mode of the field labeled  $a$  and  $b$  [11] with not only the self-coupling term exists [12] but also so-called cross-Kerr coupling is taken into account [10,15]. The Hamiltonian comprising all above- terms which describes the dynamics of the our system can be written as (assuming  $\hbar = 1$ ):

$$\hat{H} = \hat{H}_{free} + \hat{H}_{nl} + \hat{H}_{int} \tag{1}$$

Where

$$\hat{H}_{free} = \omega_a \hat{a}^\dagger \hat{a} + \omega_b \hat{b}^\dagger \hat{b} \tag{2}$$

is free renormalized Hamiltonian,

$$\hat{H}_{nl} = \frac{\chi_a}{2} \hat{a}^{\dagger 2} \hat{a}^2 + \frac{\chi_b}{2} \hat{b}^{\dagger 2} \hat{b}^2 + \tilde{\chi} \hat{a}^\dagger \hat{a} \hat{b}^\dagger \hat{b} \tag{3}$$

describes Kerr-like media (involving cross-Kerr coupling), and

$$\hat{H}_{int} = \varepsilon \hat{a}^{\dagger 2} \hat{b}^2 + \varepsilon^* \hat{b}^{\dagger 2} \hat{a}^2 \tag{4}$$

corresponds to the nonlinear interaction between two modes of the field.

The parameters  $\chi_a$  ( $\chi_b$ ) are proportional to the third-order susceptibility,  $\tilde{\chi}$  describes the cross-action process, whereas  $\varepsilon$  means the strength of the nonlinear interaction. Since Hamiltonian system is expressed in term of bosonic creation and annihilation operators, we can present them as square matrices, for example of mode  $a$ :

$$\hat{a}^\dagger = \begin{bmatrix} 0 & 0 & 0 & \dots & 0 & 0 \\ 1 & 0 & 0 & \dots & 0 & 0 \\ 0 & \sqrt{2} & 0 & \dots & 0 & 0 \\ \vdots & \vdots & \vdots & \ddots & \vdots & \dots \\ 0 & 0 & 0 & \dots & \sqrt{n-1} & 0 \end{bmatrix} \tag{5}$$

$$\hat{a} = \begin{bmatrix} 0 & 1 & 0 & \dots & 0 & 0 \\ 0 & 0 & \sqrt{2} & \dots & 0 & 0 \\ \vdots & \vdots & \vdots & \ddots & \vdots & \dots \\ 0 & 0 & 0 & \dots & 0 & \sqrt{n-1} \\ 0 & 0 & 0 & \dots & 0 & 0 \end{bmatrix}. \quad (6)$$

The creation (annihilation) operator  $\hat{b}^\dagger$  ( $\hat{b}$ ) for mode  $b$  can be also constructed by the same way. Assuming that the field was initially in the Glauber coherent states for the both modes as:

$$|\psi(0)\rangle = |\alpha\rangle \otimes |\beta\rangle \quad (7)$$

Obviously, it is possible to construct those coherent states in Fock basis as:

$$|\alpha\rangle = e^{-\frac{|\alpha|^2}{2}} \sum_{n_a=0}^{\infty} \frac{\alpha^{n_a}}{\sqrt{n_a!}} |n_a\rangle; \quad |\beta\rangle = e^{-\frac{|\beta|^2}{2}} \sum_{n_b=0}^{\infty} \frac{\beta^{n_b}}{\sqrt{n_b!}} |n_b\rangle \quad (8)$$

where  $\alpha$  and  $\beta$  are equal to the mean number of photon by the following relation  $\langle \hat{n}_a \rangle = \langle \hat{a}^\dagger \hat{a} \rangle = |\alpha|^2$  and  $\langle \hat{n}_b \rangle = \langle \hat{b}^\dagger \hat{b} \rangle = |\beta|^2$ . In consequence, we can easily express these states in the matrix presentation.

The aim of our consideration is to check how interaction with external bath can influence on nonclassical properties generation.

When the system is influenced by external bath, time-evolution of our system is described by the density matrix, which is a solution of the master equation, within the standard Markov approximation [4] as:

$$\frac{d\hat{\rho}}{dt} = -i(\hat{H}\hat{\rho} - \hat{\rho}\hat{H}) + \hat{L}_{loss}^{(a)}\hat{\rho} + \hat{L}_{loss}^{(b)}\hat{\rho}, \quad (9)$$

where appearing here Liouvillian of two-mode density matrix  $\hat{\rho}$  are given by

$$\hat{L}_{loss}^{(a)}\hat{\rho} = \frac{\gamma_a}{2} \left( [\hat{a}\hat{\rho}, \hat{a}^\dagger] + [\hat{a}, \hat{\rho}\hat{a}^\dagger] \right) + \gamma_a \bar{n}_a [\hat{a}, \hat{\rho}], \hat{a}^\dagger \quad (10)$$

$$\hat{L}_{loss}^{(b)}\hat{\rho} = \frac{\gamma_b}{2} \left( [\hat{b}\hat{\rho}, \hat{b}^\dagger] + [\hat{b}, \hat{\rho}\hat{b}^\dagger] \right) + \gamma_b \bar{n}_b [\hat{b}, \hat{\rho}], \hat{b}^\dagger \quad (11)$$

caused by amplitude damping [4]. The parameter  $\gamma_i$  ( $i=a,b$ ) is damping constants, whereas  $\bar{n}_i$  ( $i=a,b$ ) denotes the mean number of photon in thermal bath. Note that we have quiet “reservoirs” at zero temperature corresponding to the case  $\bar{n}_a = \bar{n}_b = 0$ , and noisy “reservoirs” when the temperature is greater than zero corresponding to  $\bar{n}_a, \bar{n}_b > 0$ .

Thank to *quantum Monte Carlo*, it is possible to solve operator equation (9) by appropriate standard numerical simulation using calculation of matrix exponentials and

advantage of considering super operators. Matlab computing language [16] is a appropriate software for performing our purposes due to their simplicity and ease of use even for computer users who are not very experienced in numerical calculations.

### 3. The existence of nonclassical properties

#### 3.1. Squeezing and higher-order squeezing effect

In order to investigate the single mode squeezing effect we define quadrature variances and principal squeezing variances [14,22] as:

$$\left\{ \begin{matrix} S_a \\ S'_a \end{matrix} \right\} = \frac{1}{2} \left[ \left\langle \Delta \hat{a}^\dagger \Delta \hat{a} \right\rangle \pm \text{Re} \left\langle \left( \Delta \hat{a}^2 \right) \right\rangle \right] \quad (12)$$

$$\lambda_a = \frac{1}{2} \left[ \left\langle \Delta \hat{a}^\dagger \Delta \hat{a} \right\rangle - \left| \left\langle \left( \Delta \hat{a}^2 \right) \right\rangle \right| \right] \quad (13)$$

where the fluctuation of operators are defined as

$$\left\langle \Delta \hat{X} \Delta \hat{Y} \right\rangle = \left\langle \hat{X} \hat{Y} \right\rangle - \left\langle \hat{X} \right\rangle \left\langle \hat{Y} \right\rangle \quad (14)$$

The expectation value can be calculated from density matrix as

$$\left\langle \hat{X} \right\rangle = \text{Tr} \left( \hat{\rho} \hat{X} \right) \quad (15)$$

Two mode squeezing can be defined from two mode quadrature variances and principal squeezing as [9]:

$$\left\{ \begin{matrix} S_{ab} \\ S'_{ab} \end{matrix} \right\} = 2 \left[ 1 + \left\langle \Delta \hat{a}^\dagger \Delta \hat{a} \right\rangle + \left\langle \Delta \hat{b}^\dagger \Delta \hat{b} \right\rangle + 2 \text{Re} \left\langle \Delta \hat{a}^\dagger \Delta \hat{b} \right\rangle \pm \text{Re} \left\langle \left( \Delta \hat{a}^2 \right) \right\rangle + \left\langle \left( \Delta \hat{b}^2 \right) \right\rangle + 2 \left\langle \Delta \hat{a}^\dagger \Delta \hat{b} \right\rangle \right] \quad (16)$$

$$\lambda_{ab} = 2 \left[ 1 + \left\langle \Delta \hat{a}^\dagger \Delta \hat{a} \right\rangle + \left\langle \Delta \hat{b}^\dagger \Delta \hat{b} \right\rangle + 2 \text{Re} \left\langle \Delta \hat{a}^\dagger \Delta \hat{b} \right\rangle + \left| \left\langle \left( \Delta \hat{a}^2 \right) \right\rangle + \left\langle \left( \Delta \hat{b}^2 \right) \right\rangle + 2 \left\langle \Delta \hat{a}^\dagger \Delta \hat{b} \right\rangle \right| \right] \quad (17)$$

One mode squeezing can be detected when quadrature variances and principal squeezing go below zero [8] and two mode squeezing can be observed in a quantum system if the two mode quadrature variances and principal squeezing are smaller than 2 [9]. In the Fig.1 we show the time-evolution of the squeezing parameters  $S_{a(b)}$ ,  $S'_{a(b)}$  and that of principal squeezing  $\lambda_{a(b)}$  for single mode. For the chosen values of the parameters, squeezing cannot be created in  $S'_{a(b)}$  factors. Assuming that the amplitude of the initial coherent states  $\alpha$  and  $\beta$  are real and equal to each other. Because of the equivalence, the lines for two modes are identical. From the behavior of squeezing factors and principle squeezing, we see that despite of effect of dissipation process, our system can give single mode squeezing in both modes  $a$  and  $b$ .

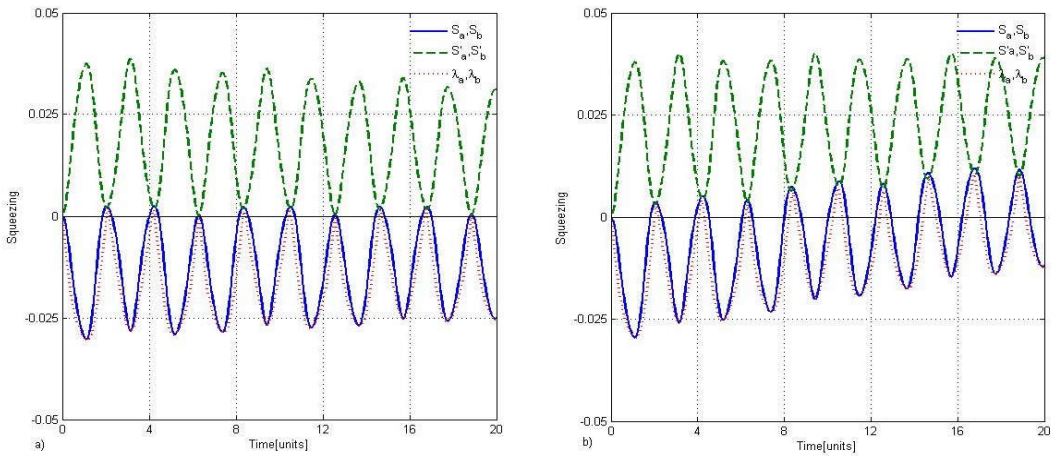


**Figure 1.** Evolution of one mode squeezing factor when initial coherent states are  $\alpha = 0.2, \beta = 0.2$ , other parameters  $\chi_a/2 = \chi_b/2 = \tilde{\chi} = 1, \varepsilon = 0.5, \gamma = 0.001$ . We assume that  $\bar{n}_a = \bar{n}_b = 0$  in Figure a) and  $\bar{n}_a = \bar{n}_b = 0.1$  in Figure b)

In the Figure 2 two-mode quadrature variances  $S_{ab}, S'_{ab}$  and two-mode principle squeezing  $\lambda_{ab}$  are plotted. For the initial coherent states  $\alpha=0.2, \beta=0.2$ , we see that the quadrature  $S'_{ab}$  does not give any signature of squeezing, contrary to  $S_{ab}$  and  $\lambda_{ab}$  which appear with a quite high intensity. Additionally, with non-zero temperature bath, one and two-mode squeezing decay very slow in the time domain. Of course, when  $\bar{n}_a = \bar{n}_b = 0.1$ , squeezing effects degenerate faster than for non-zero temperature bath, we can conclude that our system is more sensitive with nonzero temperature bath.

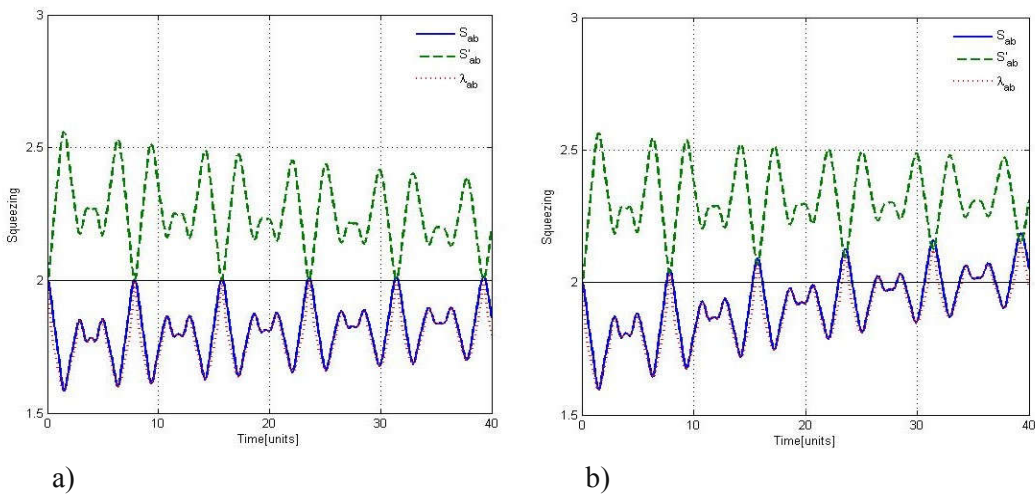


**Figure 2.** The time-evolution of two-mode quadrature variances when initial coherent states are  $\alpha = 0.2, \beta = 0.2$ , other parameters  $\chi_a/2 = \chi_b/2 = 1; \tilde{\chi} = 1, \varepsilon = 0.5, \gamma = 0.001$ . We assume that  $\bar{n}_a = \bar{n}_b = 0$  in Figure a) and  $\bar{n}_a = \bar{n}_b = 0.1$  in Figure b)

One-and two-mode squeezing are widely applied in the literatures. However, they can be treated as the lowest order nonclassicality indicators, whereas there appear other criteria which are can be applied to test *higher-order squeezing* effect. In our consideration, for convenience we use the definition given by Hillery [5], that provides witness for the existence of higher-order nonclassicality through the two amplitude powered quadrature variables defined with use of higher power of creation and annihilation operators as:

$$\hat{X}_{1,a} = \frac{\hat{a}^k + \hat{a}^{\dagger k}}{2}, \quad \hat{X}_{2,a} = i \frac{\hat{a}^{\dagger k} - \hat{a}^k}{2} \quad (18)$$

for the mode  $a$ , where  $k$  is a positive integer. Since two operators  $\hat{X}$  and  $\hat{Y}$  do not commute, from uncertainty relation, we can obtain a condition of higher-order squeezing:

$$\left\{ \begin{matrix} H_{1,a} \\ H_{2,a} \end{matrix} \right\} = \left\langle \left( \Delta \hat{X}_{j,a} \right)^2 \right\rangle - \frac{1}{2} \left| \left\langle \hat{Z} \right\rangle \right|^2 < 0, \quad (19)$$

where  $j = \{1, 2\}$  and  $[\hat{X}_{1,a}, \hat{X}_{2,a}] = i\hat{Z}$ . Of course, we obtain similarly the condition of higher-order squeezing for mode b.

Time-evolution of  $H_{1,a}(H_{1,b})$  and  $H_{2,a}(H_{2,b})$  are plotted in Figure 3 to seek for the signal of higher order squeezing. From this figure, where negative parts of the plots depict signature of higher-order squeezing we can recognize that this nonclassical properties are present for the both: zero- and non-zero temperature bath. Of course, one can see that the effect of damping is more evident for the case depicted at the right-hand plots where the negative parts predominate.

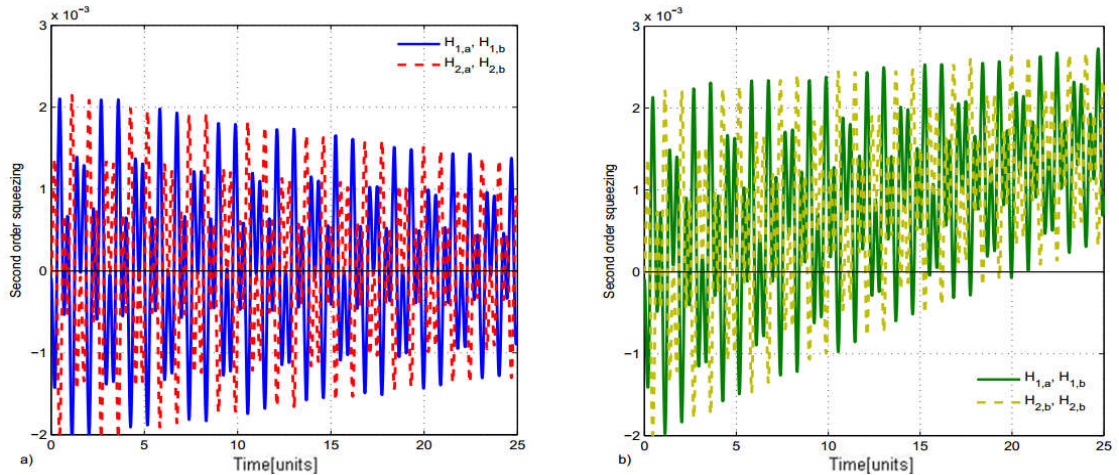


**Figure 3.** The time-evolution of  $H_{1,a}(H_{1,b})$  (solid line), and  $H_{2,a}(H_{2,b})$  (dashed line) when initial coherent states are  $\alpha = \beta = 0.2$ , other parameters  $\chi_a/2 = \chi_b/2 = 1$ ;  $\tilde{\chi} = 1$ ,  $\varepsilon = 0.5$ ,  $\gamma = 0.001$ . We assume that  $\bar{n}_a = \bar{n}_b = 0$  in Figure a) and  $\bar{n}_a = \bar{n}_b = 0.1$  in Figure b)

### 3.2. Antibunching and higher-order antibunching

In quantum statistics, signatures of the single-mode case photon antibunching can be obtained in terms of the correlation function [15], later defined in terms of the creation and annihilation operators as:

$$D_a^2 = \langle \hat{a}^{\dagger 2} \hat{a}^2 \rangle - \langle \hat{a}^\dagger \hat{a} \rangle^2 < 0. \tag{20}$$

More general the criteria to investigate the higher-order antibunching of the pure modes was first introduced by C.T.Lee [13], and afterwards was simply expressed by Pathak and Garcia [17] as

$$D_a^k = \langle \hat{a}^{\dagger k} \hat{a}^k \rangle - \langle \hat{a}^\dagger \hat{a} \rangle^k < 0. \tag{21}$$

When  $k=2$  we return to the normal antibunching.

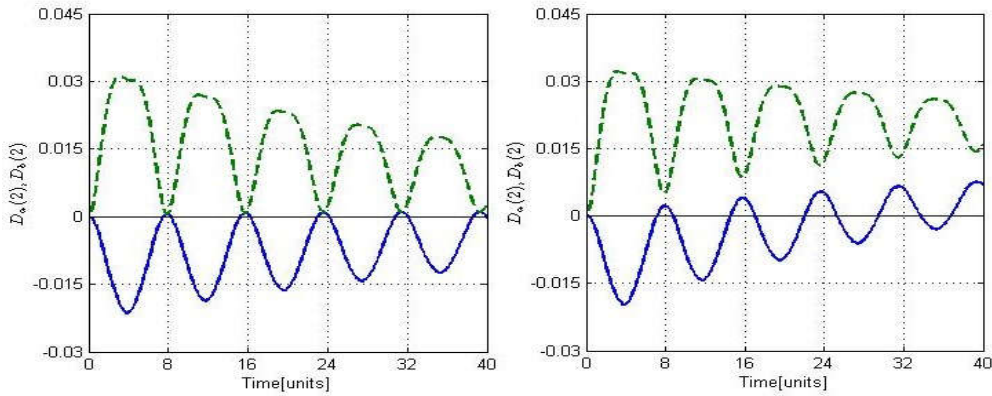


**Figure 4.** The time-evolution of  $D_a(2)$  (solid line), and  $D_b(2)$  (dashed line) when damping effects are assumed. The parameters are  $\chi_a/2 = \chi_b/2 = 1$ ;  $\tilde{\chi} = 1$ ,  $\varepsilon = 0.5$ ,  $\gamma = 0.001$ ,  $\alpha = 0.2$ ,  $\beta = 0.2$   $\bar{n}_a = \bar{n}_b = 0$  in Figure a) and  $\bar{n}_a = \bar{n}_b = 0.1$  in Figure b)

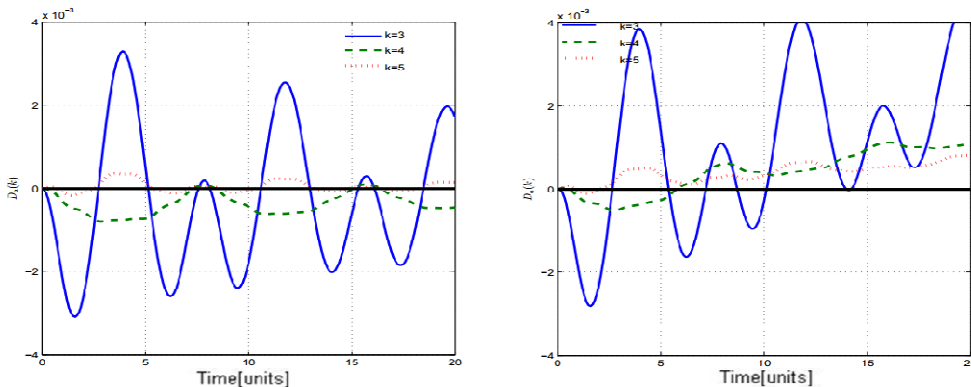


**Figure 5.** The time-evolution of  $D_a(3)$  (solid line), and  $D_b(4)$  for  $k=4$  (dashed line) when damping effects are assumed. The parameters are the same as those for Figure 4

When the coherent single modes are equal ( $\alpha=\beta$ ), there does not exist any signature of normal and higher-order antibunching. If two initial coherent states are not equal, these effects might be pronounced. The existence of the normal and higher order antibunching in our system are shown in the Figure 4 and the Figure 5. From two figures, we can not observe any normal- and higher-order antibunching in mode  $b$  when the value of  $\beta$  is smaller than that of  $\alpha$ . It is easy to recognize that for our system, this nonclassical property is evident when the initial states are setting up with smaller values of mean number of photons. The figures also illustrate the influence of damping processes due to the degeneration of  $D_a$  factor. For the case of the non-zero temperature bath, this factor is decayed faster.

### 3.3. Intermodal entanglement

There exist several entanglement criteria which would be directly applicable for multimode problems expressed in terms of expectation values of field operators. Among them, Hillery-Zubairy (HZ) criteria I and II [2,7] have obtained more attention due to simple computation, experimental practicability and their recent success in observing entanglement in various physical system. The HZ-I criterion can be generally expressed in terms of the creation and annihilation operators in the following way [8]:

$$E_{ab}^{kl} = \langle \hat{a}^{\dagger k} \hat{a}^k \hat{b}^{\dagger l} \hat{b}^l \rangle - \left| \langle \hat{a}^k \hat{b}^{\dagger l} \rangle \right|^2 < 0 \tag{23}$$

The HZ-II criterion, which is fulfilled for the separability states can be generalized for higher-order moments as [8]:

$$E_{ab}^{\prime kl} = \langle \hat{a}^{\dagger k} \hat{a}^k \rangle \langle \hat{b}^{\dagger l} \hat{b}^l \rangle - \left| \langle \hat{a}^k \hat{b}^l \rangle \right|^2 < 0 \tag{24}$$

When one of these inequalities is fulfilled, the multimode system is entangled.

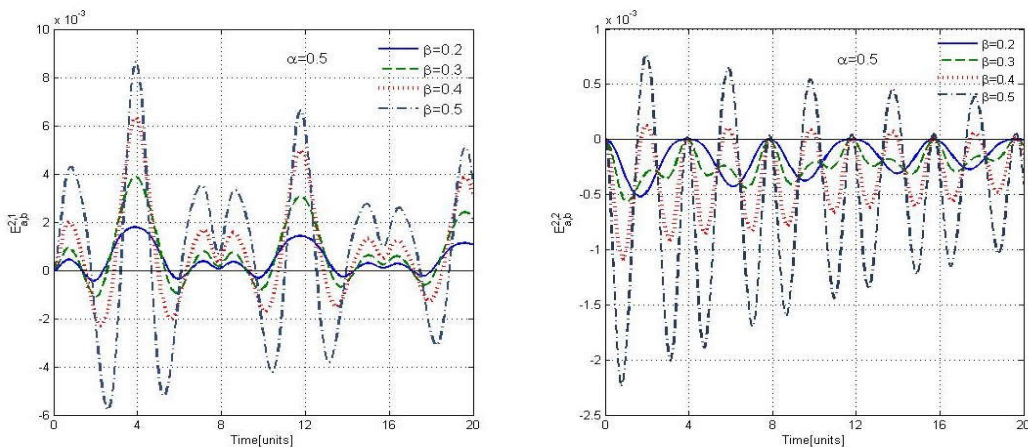


**Figure 6.** The time evolution of  $E_{ab}^{2,1}$  (a) and  $E_{ab}^{2,2}$  (b) in the presence of damping effects. The parameters are  $\chi_a/2 = \chi_b/2 = 1$ ;  $\tilde{\chi} = 1.6$ ,  $\varepsilon = 0.5$ ,  $\gamma = 0.001$ ,  $\bar{n}_a = \bar{n}_b = 0$ . The initial coherent state is described by  $\alpha = 0.5$ ,  $\beta = 0.2$  (solid line),  $\beta = 0.3$  (dashed line),  $\beta = 0.4$  (dotted line),  $\beta = 0.5$  (dash-dotted line)

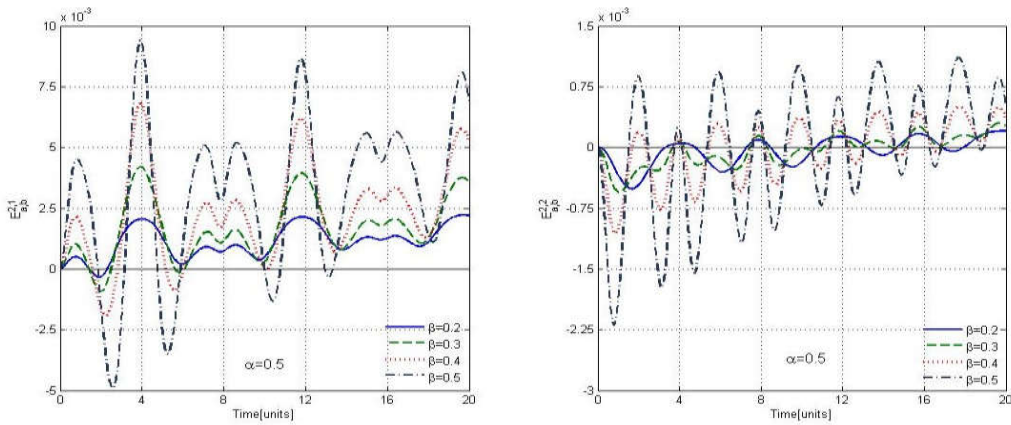


**Figure 7.** The time evolution of  $E_{ab}^{2,1}$  (a) and  $E_{ab}^{2,2}$  (b) the same as Figure 6 but for  $\bar{n}_a = \bar{n}_b = 0.1$

The plots of factors showing the existence of intermodal entanglement in coupled-mode influenced by damping processes are shown in Figure 6 and Figure 7. The negative parts of the plots  $E_{ab}^{2,1}$  and  $E_{ab}^{2,2}$  show us that higher-order intermodal entanglement is present in our system. Also, we observe that the deeper minima appear for the greater values of the parameters  $\alpha$  and  $\beta$  determining initial coherent states. For the case of the non-zero temperature bath, the deterioration of the entanglement is faster than of zero one. Furthermore, it is not possible to detect the signatures of lowest and higher intermodal entanglement by using (24) criterion. Therefore, one can say that our Kerr-like coupler system including nonlinear interaction term is sensitive for the interaction with environment, but still it can be seen as a source of intermodal entanglement and its higher orders.

#### 4. Conclusions

Various types of nonclassical effects in the model of the nonlinear Kerr-coupler such as squeezing, antibunching, inter-mode entanglement and their higher order counterparts have been observed. Using unitary evolution operator formalism we simulated quantum dynamics of system and found numerically the “exact” solutions for these factors under damping effect. We showed that despite of interacting with environment, the parameters considered here can be an indicator of the generation such nonclassical effects and hence, quantumness of the system. Additionally, it was easy to recognize that under the effect of damping, those properties do not exist for some of parameters, but can be generated with small value of mean number of photons for the initial coherent states.

#### References

- [1] Bennett C H and Wiesner S J. (1992), *Phys. Rev. Lett.* 69 2881-2884.
- [2] Duan L M, Giedke G, Cirac J I and Zoller P. (2000), *Phys. Rev. Lett.* 84 2722-2725.

- [3] Ekert A. (1991), *Phys. Rev. Lett.* 67 661.
- [4] Gardiner C W, Zoller P. (2000), *Quantum Noise*. Springer-Verlag 3rd ed.
- [5] Hillery M. (1987), *Phys. Rev. A* 36 37968.
- [6] Hillery M. (2000), *Phys. Rev. A* 61 022309.
- [7] Hillery M and Zubairy M S. (2006), *Phys. Rev. A* 74 032333.
- [8] Hillery M and Zubairy M S. (2006), *Phys. Rev. Lett.* 96 050503.
- [9] Karska M and Perina J. (1990), *J. Mod. Opt.* 37 195.
- [10] Kowalewska-Kudlaszyk A. (2013), *Phys. Scr.* T153 01403.
- [11] Korolkova N, Perina J. (1997), *Opt. Commun.* 136 135.
- [12] Kowalewska-Kudlaszyk A, Leonski W, Thi Nguyen D, Cao Long Van (2014), *Phys. Scr.* T160 014023.
- [13] Lee C T (1990), *Phys. Rev. A.* 41 1569; 1721.
- [14] Luks A, Perinova V and Perina J. (1988), *Opt. Commun.* 67 149-151.
- [15] Mandel L and Wolf E. (1995), *Optical Coherence and Quantum Optics*. Cambridge, New York.
- [16] Matlab documentation, available at: <http://www.mathworks.com/help/matlab/index.html>
- [17] Pathak A and Garcia M. (2006), *Applied Physics B* 84, 484.
- [18] Perinova V, Luks A, and Krapelka J. (2013), *J. Phys. B: At. Mol. Opt. Phys.*, 46 195301.
- [19] Stobinska M, Jeong H, and Ralph T C. (2007), *Phys. Rev. A*, 75 052105.
- [20] Stobinska M, Milburn G J, and Wodkiewicz K. (2008), *Phys. Rev. A*, 78 013810.
- [21] Stobinska M, Villar A S, and Leuchs G. (2011), *EPL (Europhysics Letters)*, 94(5) 54002.
- [22] Tanas R, Miranowicz A and Kielich S. (1991), *Phys. Rev. A* 43 4014.
- [23] Yuan Z, Kardynal B E, Stevenson R M, Shields A J, Lobo C J, Cooper K, Beattie N S, Ritchie D A and Pepper M. (2002), *Science* 295 102.